Retail Market Equilibrium and Interactions among Reconfigurable Networked Microgrids

Esmaeili, Saeid ; Anvari-Moghaddam, Amjad; Jadid, Shahram

Published in:
Sustainable Cities and Society

DOI (link to publication from Publisher):
10.1016/j.scs.2019.101628

Publication date:
2019

Document Version
Accepted author manuscript, peer reviewed version

Citation for published version (APA):
Esmaeili, S., Anvari-Moghaddam, A., & Jadid, S. (2019). Retail Market Equilibrium and Interactions among Reconfigurable Networked Microgrids. *Sustainable Cities and Society*, *49*, [101628]. https://doi.org/10.1016/j.scs.2019.101628

Accepted Manuscript

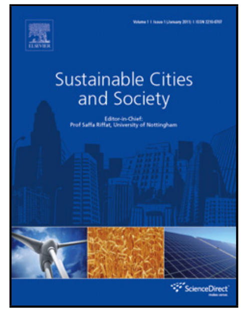

Title: Retail Market Equilibrium and Interactions among Reconfigurable Networked Microgrids

Authors: Saeid Esmaeili, Amjad Anvari-Moghaddam, Shahram Jadid

PII:	S2210-6707(19)30258-6
DOI:	https://doi.org/10.1016/j.scs.2019.101628
Article Number:	101628
Reference:	SCS 101628
To appear in:	
Received date:	28 January 2019
Revised date:	23 May 2019
Accepted date:	24 May 2019

Please cite this article as: Esmaeili S, Anvari-Moghaddam A, Jadid S, Retail Market Equilibrium and Interactions among Reconfigurable Networked Microgrids, *Sustainable Cities and Society* (2019), https://doi.org/10.1016/j.scs.2019.101628

Retail Market Equilibrium and Interactions among Reconfigurable Networked Microgrids

Saeid Esmaeili [a], Amjad Anvari-Moghaddam [b], Shahram Jadid [c]

[a,c] Department of Electrical Engineering, Iran University of Science and Technology, Tehran, Iran
[b] Department of Energy Technology, Aalborg University, Aalborg, Denmark
[a] Author to whom correspondence should be addressed. Email: s_esmaeili@elec.iust.ac.ir
[b] Email: aam@et.aau.dk
[c] Email: jadid@iust.ac.ir

Highlights:

- A multi-follower-type bi-level operation scheduling model is proposed.
- Modeling a day-ahead decision-making of reconfigurable networked microgrids.
- Investigating the effect of DLR constraint on the decision-making process.
- Developing an advanced retail electricity market among the competing players.

Abstract

In this paper, a retail market equilibrium among a set of competing players, i.e., retailers and Microgrids (MGs), considering Dynamic Line Rating (DLR) constraint and demand response (DR) actions is modeled. In this regard, a multi-follower-type bi-level optimization scheduling for decision making of Distribution System Operator (DSO) and reconfigurable networked MGs with inherently conflicting objectives is presented. In this model, the upper-level player of the Main Problem (MP) minimizes the total cost from DSO's perspective, while in the lower-level of the MP, networked MGs compete with retailers in the retail electricity market as an interior Sub Problem (SP). In the upper-level of the SP the profit of each MG is maximized, where in the lower-level of the SP the social welfare of the retail market clearing process is maximized. Since the resulting bi-level problem is nonlinear and non-convex, it is transformed into a single-level Mixed-Integer Second-Order Cone Programming (MISOCP) problem using Karush–Kuhn–Tucker (KKT) optimality conditions and linearization techniques. The effectiveness of the proposed model is investigated on a real-test system in both grid-connected and islanded modes under different scenarios.

Key words: Bi-level optimization, Hourly reconfiguration, Networked microgrids, Operation scheduling, Retail market.

Nomenclature

t / br / RCS	Indices for time/ branches/ RCSs.	$h_{i,\zeta}$	Amount of curtailed power for the ζ^{th} step of DR program in bus i.
i, j	Index of buses ($i, j = 1, 2, ..., \mathrm{N}_{bus}$).	$E_{i,t}$	The energy level of ESS i at time t (MWh).
p, q	Index of MGs ($p, q = 1, 2, ..., \mathrm{N}_{MG}$).	η_i^{ch} / η_i^{dch}	Charging/discharging efficiency of ESS i.

ξ	Index of steps in bid-quantity package offers for DR participations ($\xi = 1, 2, 3, ..., \varphi$).
w	Index of retailers ($w = 1, 2, ..., N_{retailer}$).
C_t^{loss} / C_t^{RCS}	Costs related to power losses/ switching of RCSs at time *t* ($).
C_t^{WM}	Cost of exchanging power with the wholesale market at time *t* ($).
C_t^{MG2DSO}	Cost of exchanging power between DSO and MGs ($).
ρ^{loss} / ρ^{RCS}	Hourly power loss ($/MWh) /switching price ($).
$\rho_t^{WM} / \rho_t^{RM}$	Hourly wholesale/retail market price ($/MWh).
$N_{br} / N_{bus} / N_{sub}$	Number of branches/ buses/ substations in the distribution system.
$N_{\max}^{RCS}$	Maximum allowable switching actions.
$\alpha_i^{MT}, \beta_i^{MT}$	Cost coefficients of MT *i* ($/MW), ($).
$\alpha_i^{PV}, \beta_i^{PV}$	Cost coefficients of PV *i* ($/MW), ($).
$\alpha_i^{ESS}, \beta_i^{ESS}$	Cost coefficients of ESS *i* ($/MW), ($).
$U_{i,t}^{ch} / U_{i,t}^{dch}$	Binary variable for the charging/discharging status of ESS *i* that is equal to 1 if ESS *i* is in the charging/discharging mode at time *t*.
α_{solar}	Solar absorptivity.
Q_{se}	Radiated heat intensity by sun.
mc_P	Heat capacity of conductor (J/m- ℃)
T_{ave}	Average temperature of conductor (℃)
T_a, T_s	Ambient air temperature, conductor surface temperature (℃)
$T_{br,t}$	Temperature of conductor at time *t* (℃).
ρ_f, D_0	Air density (kg/m^3), conductor diameter (cm^2).
V_w	Wind speed (m/s).
K_f	Thermal conductivity of the system (W/ (cm. ℃)).
ε	Emissivity (W/m^2).
A	Area of the conductor (m^2).
$E_i^{initial}$	Initial stored energy in ESS *i* (MWh).

$R(T_{ave})$	AC resistance of conductor at the average temperature (Ω/m).
$I_{ij,t}$	Current of line *ij* at time *t* (kA).
$X_{RCS,t}$	Binary variable for the status of RCSs (1 if the RCS is closed and 0, otherwise).
$Pr_{p,t}^{\phi}$	Profit related to term ϕ ($) (ϕ includes loads, MTs, PVs, DR participations, retailers, exchanged power among MGs, and exchanged power between MGs and DSO).
P_t^{loss}	Total power losses at time *t* (MW).
$P_t^{DSO2WM} / P_t^{WM2DSO}$	Sold/ purchased power to/from wholesale market at time *t* by DSO (MW).
$P_t^{DSO2MGp} / P_t^{MGp2DSO}$	Transmitted power from DSO to MG *p* / from MG *p* to DSO (MW).
$P_{t,s}^{MGp2MGq}$	Transmitted power from MG *p* to MG *q* at time *t* (MW).
P_t^{Rw2MGp}	Transmitted power from retailer *w* to MG *p* at time *t* (MW).
$P_{i,t}^{PV}$	Hourly Output power of PV *i* (MW).
$P_{i,t}^{MT}, Q_{i,t}^{MT}$	Hourly Output active/reactive power of MT *i* (MW), (MVAR).
$P_{i,t}^{ch} / P_{i,t}^{dch}$	Charged/discharged power of ESS *i* at time *t* (MW).
$P_{i,t}^{DR}$	Total curtailed power of DR for bus *i* at time *t* (MW).
$P_{i,t}^{L}$	Amount of electrical load for bus *i* at time *t* (MW).
$P_t^{MGp,bid/offer}$	The clearing quantity of MG *p* at time *t* (Positive/negative values are assigned for bidding/offering mode) (MW).
P_t^{Rw}	The clearing quantity of retailer *w* at time *t* (MW).
$q_{c,br,t} / q_{r,br,t}$	Convection/ radiated heat loss (W/m).
$q_{s,br,t}$	Heat gain from sun (W/m).
$Z_C / Z_L / H_C$	Azimuth of the sun (gradian) /azimuth of the line (gradian) /altitude of the sun (gradian).
$V_{i,t}$	Voltage magnitude of bus *i* at time *t* (V).
Z_{ij} / y_i	Impedance of line *ij* (Ω) /admittance between bus *i* and the ground (S).
$S_{ij,t}$	Apparent power for line *ij* at time *t* (VA).
g_i / b_i	Conductance/ susceptance of bus *i* (S).

$\lambda_{p,t}^{MG}$	Bid/offer price of MG p at time t (\$/MWh).	r_{ij} / x_{ij}	Resistance/reactance of line ij (Ω).
$P_{i,t}, Q_{i,t}$	The net amount of injected active/reactive power at bus i (MW), (MVAR).	$\lambda_{w,t}^{R}$	Offer price of retailer w at time t (\$/MWh).

1. Introduction

Over the past decade, Distributed Energy Resources (DERs) including dispatchable and renewable sources have drawn the attention of researchers since they are a promising solution to address the energy crisis and environmental deteriorations. One of the particular paradigm in optimal control of energy resources is the so-called networked Microgrids (MGs). They are autonomous and generally privately-owned clusters of DERs, Energy Storage Systems (ESSs), and loads [1], which can transact energy among each other and/or with the distribution network (through coordination of a system operator) to meet MG owners' (MGOs') objectives. It is demonstrated [2] in that the networked MGs possess the capability of increasing network reliability and decreasing the total operation cost compared to the individual MGs. The optimal operation scheduling of the individual MG from various viewpoints has been extensively investigated so far [3]-[4]. In [5], an optimal economic operation of networked MGs has been proposed using particle swarm optimization algorithm. To maximize the financial profit of each coalition in networked MGs, a cooperative energy and reserve scheduling framework for optimal operation of MGs has been modeled in [6]. An optimal energy management of networked MGs has been formulated in [7] as a Mixed Integer Linear Programming (MILP) problem, where the energy trading is allowed not only externally with the upstream grid, but also internally among neighboring MGs.

In [5]-[7], distribution system operator (DSO) and MGOs are not considered as independent entities, where in [8] a bi-level operation scheduling of DSO and MGs as the self-governing stakeholders with their individual objectives has been modeled. In the upper-level problem, the optimal operation strategies of DERs in distribution system have been determined to minimize voltage deviation and power losses, where the lower-level optimization problem minimizes the total operating cost of MGs. In [9], a bi-level decentralized Distribution Management System (DMS) for the coordinated energy scheduling of networked MGs in a distribution system for both grid-connected and islanded modes has been studied. To demonstrate the effectiveness of the proposed bi-level framework, a modified IEEE 33-bus distribution network with three MGs has been used. However, the interactions between the upper and lower-levels were not taken into account in the proposed models in [8]-[9]. To address this issue, authors of [10] introduce a bi-level operation scheduling of DERs in distribution system considering the interaction between DSO and MGs. The intended multi-follower decision-making problem seeks to minimize the DSO's operation cost taking into account the maximizing the profit of each MG. The Karush–Kuhn–Tucker (KKT) optimality conditions of the lower-level problem are then used to transform the bi-level optimization problem into a single-level problem. Likewise, in [11]-[12], a hierarchical bi-level decision-making framework for optimal operation of DSO and networked MGs has been proposed.

Due to the growing share of new players such as prosumers in local and regional electricity networks, a retail electricity market with new functionalities and pricing mechanism should be introduced. Regarding the reviewed literature, the major drawback lies within the lack of such energy-trading floor to facilitate the power exchange process considering social well fare. Marzband, et al. [13] present a retail electricity market framework based on the non-cooperative gaming structure for the optimal operation of residential MGs in a distribution system. To fill the gap between DSO and MGOs as the major players of the distribution sector, [14] develops an advanced retail electricity market for day-ahead energy exchange commitments. In [15], virtual power plants compete with retailers by submitting price-quantity bids/offers in the established advanced retail market platform. The upper-level problem maximizes the profit of each virtual power plant, where the lower-level problem maximizes social welfare of the retail market clearing process. However, the interactions between DSO and virtual power plants are not considered and the problem is tackled from virtual power plants' viewpoint. To the best of our knowledge, none of the reviewed literature presents a retail electricity market in the DSO-MGOs gaming strategy.

From another perspective, a flexible fashion of distribution networks is envisioned in recent years by utilizing Remotely Controlled Switches (RCSs) in short-term operation scheduling [16]-[17]. The multi-objective day-ahead scheduling of networked MGs in conjunction with hourly reconfiguration in distribution system has been proposed in [18]. Total cost and emission reduction and power quality enhancement have been treated as the objective functions of the problem. Authors in [19] present a simultaneous operation scheduling and hourly reconfiguration model in a distribution system considering Responsive Loads (RLs), where the proposed optimization problem is solved by particle swarm optimization algorithm. While the previous research works address several operation challenges from various technical aspects, Dynamic Line Rating (DLR) constraint has not been considered in their models. Technically, DLR is a practical constraint that dynamically estimates line ampacity (maximum current carrying capacity of a distribution line) in real-time based on the weather condition, conductor resistance, size, and current. Due to the lower sizes of conductors in distribution systems, the DLR constraint becomes more crucial in those systems than in the transmission level [20]. Therefore, DLR plays a strategic role in operation scheduling of MGs in both grid-connected and islanded modes. Particularly, as the line current reaches its maximum thermal capacity limits in the islanded mode, DLR can be a more serious issue. In [21], an optimal operation scheduling of reconfigurable MGs considering DLR limitations has been proposed. It is demonstrated that by taking the DLR constraint into account in overhead lines of MGs, overloaded lines are detected. However, the interactions between DSO and MGs are not considered, and the retail electricity market among the multiple competing players is not established as well.

In this paper, a Nash equilibrium among a set of competing players (MGs and retailers) considering DLR and DR actions in the retail and wholesale electricity market is modeled. In this regard, a multi-follower-type bi-level optimization scheduling for decision-making of DSO and reconfigurable networked MGs is proposed. In this model, the upper-level of the Main Problem (MP) minimizes the total cost from DSO's point of view including the costs of hourly switching actions, power losses, exchanged power between DSO and MGs, and exchanged power with wholesale market. In the lower-level of the MP, networked MGs compete with retailers in the retail electricity market which is cleared by the DSO. Therefore, the lower-level entities of the MP form a gaming structure in the interior Sub Problem (SP). In the upper-level of the SP, the profit of each MG is maximized, where the lower-level of the SP maximizes the social welfare of the retail market clearing process. Since the resultant bi-level model is nonlinear and non-convex, it is transformed into a single-level Mixed-Integer Second-Order Cone Programming (MISOCP) optimization problem via KKT conditions and linearization techniques. To authenticate that each generated result is a Nash equilibrium, a single-iteration diagonalization technique is used. Moreover, the effect of hourly reconfiguration on the decision-making process of networked MGs along with DLR constraint and DR actions are investigated. Briefly, the main contributions of this paper are highlighted as follows:

- Modelling a multi-follower-type bi-level optimization scheduling for decision-making of DSO and reconfigurable networked MGs,
- Developing an advanced retail electricity market among the multiple competing players,
- Investigating the effect of DLR constraint on the decision-making process of networked MGs in distribution systems along with hourly reconfiguration and DR actions in both grid-connected and islanded modes.

The rest of the paper is organized as follows: In section 2, a conceptual framework for the proposed retail electricity market is presented. Dynamic thermal line rating based heat balance equation is formulated in section 3. Section 4, proposes the bi-level formulation of the optimization problem, while section 5 discusses the simulation results. Finally, conclusions are drawn in section 6.

2. Conceptual framework of the retail electricity market

In the envisioned deregulated market environment, a flat or Time-of-Use (TOU) energy price in retail market can cause market inefficiencies [22]-[23], as it is demonstrated for the wholesale market at the transmission network level [24]. Thus, this paper provides an advanced retail market framework. In this model, each retailer procures power from wholesale market and sells it in a retail market where MGs coexist and could transact energy locally using their own DERs and ESSs facilities. In this regard, market participants (MGs and retailers) compete with each other through submitting a set of hourly price-quantity bids/offers in the retail electricity market. DSO, as the market operator, clears the retail market for each hour (market update cycle), and finally announces the clearing price and related clearing quantity to all participants.

3. Dynamic thermal line rating based heat balance equation

Being exposed to different thermal and electrical phenomena, the behavior of a given conductors (in terms of maximum power capacity limit) can be changed dynamically rather than fixed assumptions. As shown in [25], such thermal behavior (known as DLR) might take an hour to reach the steady state at a certain conditions (such as standard wind speed). To derive DLR constraints, the heat balance equation (1) is implemented in our proposed model as follows:

$$q_{c,br,t} + q_{r,br,t} + mc_P \frac{dT_{ve}}{dt} = q_{s,br,t} + I_{br,t}^2 R(T_{ave}) \tag{1}$$

Equation (1) includes the terms of heat loss (including the convection and radiated heat loss) and heat gain, which are explained in the following.

- Heat loss:

According to the following equations, the convection heat loss is calculated for zero (natural convection), low and high wind speed rates.

$$q_{c,0,br,t} = 3.645\rho_f^{0.5} D_0^{0.75}(T_s - T_a) \tag{2}$$

$$q_{c,low,br,t} = K_{angle}\left(1.01 + 1.35\left(\frac{D_0\rho_f V_w}{\mu_f}\right)^{0.52}\right)K_f\,(T_s - T_a) \tag{3}$$

$$q_{c,high,br,t} = K_{angle}\,0.754\left(\frac{D_0\rho_f V_w}{\mu_f}\right)^{0.6} K_f\,(T_s - T_a) \tag{4}$$

where, K_{angle} reflects the wind direction considering the angle between the conductor axis and the wind direction β as follows:

$$K_{angle} = 1.194 - \cos(\beta) + 0.194\cos(2\beta) + 0.3\sin(2\beta) \tag{5}$$

Based on the IEEE standard [26], the convection heat loss rate should be chosen as the largest value among the zero, low, and high wind speed rates, stated in (6).

$$q_{c,br,t} = \max(q_{c,0,br,t}, q_{c,low,br,t}, q_{c,high,br,t}) \tag{6}$$

The second term, represented by (1), is the heat loss of conductors radiated in the surrounding atmosphere. It can be calculated by (7) as follows:

$$q_{r,br,t} = 17.8 D_0 \varepsilon\left[\left(\frac{T_s + 273}{100}\right)^4 - \left(\frac{T_a - 273}{100}\right)^4\right] \tag{7}$$

- Heat gain:

The solar heat gain rate is defined as the amount of solar heat energy that can be absorbed and delivered by a conductor. It is calculated as a function of the effective angle of incidence for the sun's ray Θ by (8).

$$q_{s,br,t} = \alpha_{solar} Q_{se}\sin(\Theta) A \tag{8}$$

$$\Theta = \arccos\left(\cos(H_C)\cos(Z_C - Z_L)\right) \tag{9}$$

Finally, by calculating (2)-(9) and considering the heat balance equation (1), the line average temperature at each time can be approximated by (10).

$$T_{br,t+1} - T_{br,t} = \frac{\Delta t}{mc_P}\left[R_{br,t} I_{br,t}^2 + q_{s,br,t} - q_{c,br,t} - q_{r,br,t}\right] \tag{10}$$

4. Bi-level formulation of the optimization problem

Bi-level problem formulation of the simultaneous operational scheduling and hourly reconfiguration of the multi-MG distribution system considering DLR and Demand Response (DR) actions is proposed in the following subsections.

4.1. Upper-level of the MP: DSO

The objective function for the upper-level of the MP, composed of four cost terms, is defined as follows:

$$OF_{DSO} = Min\left(\sum_{t=1}^{24}\left(C_t^{loss} + C_t^{RCS} + C_t^{WM} + C_t^{MG2DSO}\right)\right) \tag{11}$$

where the first term is the cost related to the power losses, which can be calculated by (12).

$$C_t^{loss} = \rho^{loss} P_t^{loss} \tag{12}$$

The amount of active power losses in (12) can be calculated by (25).

The second term, represented by (13), calculates the switching cost of RCSs at time *t*.

$$C_t^{RCS} = \rho^{RCS} \sum_{RCS=1}^{N_{RCS}} \left| X_{RCS,t} - X_{RCS,t-1} \right| \tag{13}$$

The absolute value in (13), which introduces nonlinearity can be avoided by defining new auxiliary variables $Z^{+}_{RCS,t}, Z^{-}_{RCS,t}$ as follows:

$$\begin{aligned} &X_{RCS,t} - X_{RCS,t-1} = Z_{RCS,t} \\ &Z_{RCS,t} = Z^{+}_{RCS,t} - Z^{-}_{RCS,t} \\ &\left| Z_{RCS,t} \right| = Z^{+}_{RCS,t} + Z^{-}_{RCS,t} \\ &Z^{+}_{RCS,t}, Z^{-}_{RCS,t} = 0,1 \end{aligned} \tag{14}$$

The third term in (11) denotes the cost of purchasing/selling active power from/to wholesale market by DSO represented by (15).

$$C_t^{WM} = \rho_t^{WM} (P_t^{WM2DSO} - P_t^{DSO2WM}) \tag{15}$$

Finally, the last term calculates the cost of exchanging power between MGs and DSO as follows:

$$C_t^{MG2DSO} = \rho_t^{RM} \sum_{p=1}^{N_{MG}} \left(P_t^{MGp2DSO} - P_t^{DSO2MGp} \right) \tag{16}$$

Constraints:

Constraints for the upper-level of the MP are as follows:

- *Distribution power flow equations:*

To capture the distribution power flow equations, the generic form of the branch flow model deals with the currents and powers is implemented as follows:

$$V_{i,t} - V_{j,t} = Z_{ij} I_{ij,t} \qquad \forall\ (i,j) \in br \tag{17}$$

$$S_{ij,t} = V_{i,t} I^{*}_{ij,t} \qquad \forall\ (i,j) \in br \tag{18}$$

$$\sum_{(i,j)\in br} S_{ij,t} - \sum_{(k,i)\in br} (S_{ki,t} - z_{ki} \left| I_{ki,t} \right|^2) + y_i^{*} \left| V_{i,t} \right|^2 = S_{i,t} \qquad \forall\ i = 1,2,,...,N_{bus} \tag{19}$$

where, (17) states the Ohm's law, (18) represents the branch power flow, and (19) proposes the power balance constraint at each bus. By neglecting the phase angles of voltages and currents in (19) and defining new auxiliary variables $\ell_{ij,t} = \left| I_{ij,t} \right|^2$ and $v_{i,t,s} = \left| V_{i,t,s} \right|^2$ for the squared current and voltage magnitudes, respectively, the distribution power flow equations can be derived as follows:

$$P_{i,t} = \sum_{(i,j)\in br} P_{ij,t} - \sum_{(k,i)\in br} (P_{ki,t} - r_{ki} \ell_{ki,t}) + g_i v_{i,t} \qquad \forall\ i = 1,2,,...,N_{bus} \tag{20}$$

$$Q_{i,t} = \sum_{(i,j)\in br} Q_{ij,t} - \sum_{(k,i)\in br} (Q_{ki,t} - x_{ki} \ell_{ki,t}) + b_i v_{i,t} \qquad \forall\ i = 1,2,,...,N_{bus} \tag{21}$$

$$v_{j,t} = v_{i,t} - 2(r_{ij} P_{ij,t} + x_{ij} Q_{ij,t}) + (r_{ij}^2 + x_{ij}^2) \ell_{ij,t} \qquad \forall\ (i,j) \in br \tag{22}$$

$$\ell_{ij,t} = \frac{P_{ij,t}^2 + Q_{ij,t}^2}{v_{i,t}} \qquad \forall\ (i,j) \in br \tag{23}$$

Due to the presence of quadratic terms in (23), it is still non-linear. To achieve a convex model, the equality constraint (23) can be relaxed to the following second-order cone inequality one.

$$\left\| \begin{matrix} 2P_{j,t} \\ 2Q_{j,t} \\ \ell_{ij,t} - v_{i,t} \end{matrix} \right\|_2 \le \ell_{ij,t} + v_{i,t} \qquad \forall\ (i,j) \in br \tag{24}$$

It has been proved in [27]-[28] that the proposed relaxation is exact under some mild conditions. In this paper, beside investigating the sufficient conditions proposed in [27]-[28] for the exactness of convex relaxation, the validity of the calculated optimal solution is checked in section 5.

As it is stated before, the major merit of the linear equations is their convexity to ensure the global optimality of the solutions. Finally, the amount of active power losses, utilized in (12), can be calculated by (25).

$$P_t^{loss} = \sum_{(i,j)\in br} r_{ij}\ell_{ij,t} \tag{25}$$

- *Voltage magnitude limits:*

$$V_{\min}^2 \le v_{i,t} \le V_{\max}^2 \quad , \quad v_{slack} = 1 \tag{26}$$

- *Line current limits:*

$$\ell_{ij,t} \le I_{\max}^2 \qquad \forall\ (i,j) \in br \tag{27}$$

- *DLR constraint:*

Based on (10), the temperature of each overhead line at time t should not violate its maximum allowed value as follows:

$$T_{br,t} \le T_{br,t}^{\max} \tag{28}$$

- *Exchanged power limit between the wholesale market and DSO:*

$$P_t^{WM2DSO}, P_t^{DSO2WM} \le P_{\max}^{WM2DSO} \tag{29}$$

- *Exchanged power limit between DSO and each MG:*

$$P_{\min}^{MG2DSO} \le P_t^{MGp2DSO} \le P_{\max}^{MG2DSO} \tag{30}$$

$$P_{\min}^{MG2DSO} \le P_t^{DSO2MGp} \le P_{\max}^{MG2DSO} \tag{31}$$

- *Network radiality:*

In order to guarantee the radial topology of the distribution network, (32)-(35) should be considered in the optimal reconfiguration model.

$$N_{br} = N_{bus} - N_{sub} \tag{32}$$

$$\beta_{ij} + \beta_{ji} = X_{br} \tag{33}$$

$$\beta_{0j} = 0\ , \qquad j \in N(0) \tag{34}$$

$$\sum_{j\in N(i)} \beta_{ij} = 1 \tag{35}$$

Equation (32) states that the final topology is without any loop in the equivalent tree graph. If bus *i* is the parent of bus *j* ($\beta_{ji} = 1$), or bus *j* is the parent of bus *i* ($\beta_{ij} = 1$), the related branch is in the spanning tree ($X_{br} = 1$). Equation (34) indicates that substation bus should have no parents, where (35) guarantees that the other buses should have one parent (i.e. avoiding to have islanded buses in the final configuration). It should be noted that, DSO owns the grid assets (such as overhead lines, cables, and switches), thus it operates the RCSs accordingly. DSO can utilize RCSs to reach its own objectives such as loss reduction, but it should be noted that the proposed model is a bi-level optimization problem, which each level (DSO level and MGOs level) has its own objectives. These two levels can interact with each other by the mutual variables. Thus, implementing hourly reconfiguration through RCSs can affect the final decisions made by DSO and MGOs.

- *Number of switching actions:*

$$\sum_{t=1}^{24}\left|X_{RCS,t}-X_{RCS,t-1}\right|\le N_{\max}^{RCS} \quad , \ \forall RCS=1,2,...,N_{RCS} \tag{36}$$

The absolute value in (36) introduces nonlinearity in the formulation, which can be avoided by defining new auxiliary variables as proposed in (14).

4.2. Lower-level of the MP: multi-MGs

In this level, multi-MGs compete with retailers by submitting their price-quantity bids/offers in the retail electricity market which is cleared by the DSO. Thus, the lower-level players of the MP introduce a gaming structure in the interior SP. The upper-level of the SP aims at maximizing the profit of each MG and the lower-level optimization problem maximizes the social welfare of the retail market clearing process.

4.2.1. Upper-level of the SP: maximizing the profit of each MG

$$OF_{MGp}=Max\sum_{t=1}^{24}\left(Pr_{p,t}^{L}+Pr_{t}^{MGp2DSO}+Pr_{t}^{MGp2MGq}+Pr_{p,t}^{MT}+Pr_{p,t}^{PV}+Pr_{p,t}^{ESS}+Pr_{p,t}^{R}\right) \tag{37}$$

where, the profit terms of (37) are calculated as follows:

$$Pr_{p,t}^{L}=\rho_{t}^{RM}\sum_{i\in MGp}(P_{i,t}^{L}) \tag{38}$$

$$Pr_{t}^{MGp2DSO}=\rho_{t}^{RM}\left(P_{t}^{MGp2DSO}-P_{t}^{DSO2MGp}\right) \tag{39}$$

$$Pr_{t}^{MGp2MGq}=\rho_{t}^{RM}\sum_{q=1,q\neq p}^{N_{MG}}\left(P_{t}^{MGp2MGq}-P_{t}^{MGq2MGp}\right) \tag{40}$$

$$Pr_{p,t}^{MT}=-\sum_{i\in MGp}(\alpha_{i}^{MT}P_{i,t}^{MT}+\beta_{i}^{MT}) \tag{41}$$

$$Pr_{p,t}^{PV}=-\sum_{i\in MGp}(\alpha_{i}^{PV}P_{i,t}^{PV}+\beta_{i}^{PV}) \tag{42}$$

$$Pr_{p,t}^{ESS}=-\sum_{i\in MGp}\alpha_{i}^{ESS}P_{i,t}^{ch/dch}+\beta_{i}^{ESS} \tag{43}$$

$$Pr_{p,t}^{R}=-\rho_{t}^{RM}\sum_{w\in R_{w}}(P_{t}^{Rw2MGp}) \tag{44}$$

Constraints:

The constraints for the upper-level of the SP are considered as follows:

- *Operation limit of Micro Turbines (MTs):*

$$P_{\min}^{MT}\le P_{i,t}^{MT}\le P_{\max}^{MT} \tag{45}$$

- *Exchanged power limit between DSO and each MG:*

$$P_{\min}^{MG2DSO}\le P_{t}^{MGp2DSO}\le P_{\max}^{MG2DSO} \tag{46}$$

$$P_{\min}^{DSO2MG}\le P_{t}^{DSO2MGp}\le P_{\max}^{DSO2MG} \tag{47}$$

- *Exchanged power limit between MGs:*

$$P_{\min}^{MGp2MGq} \leq P_t^{MGp2MGq} \leq P_{\max}^{MGp2MGq} \tag{48}$$

$$P_{\min}^{MG2MG} \leq P_t^{MGq2MGp} \leq P_{\max}^{MG2MG} \tag{49}$$

- *Exchanged power limit with retailers and MGs:*

$$P_{\min}^{R2MGp} \leq P_t^{Rw2MGp} \leq P_{\max}^{R2MGp} \tag{50}$$

- *Limits on operation of ESSs:*

$$P_{\min}^{ESS} U_{i,t}^{ch} \leq P_{i,t}^{ch} \leq P_{\max}^{ESS} U_{i,t}^{ch} \tag{51}$$

$$P_{\min}^{ESS} U_{i,t}^{dch} \leq P_{i,t}^{dch} \leq P_{\max}^{ESS} U_{i,t}^{dch} \tag{52}$$

$$E_{\min} \leq E_{i,t} \leq E_{\max} \tag{53}$$

$$E_{i,t} = E_{i,t-1} + \eta_i^{ch} P_{i,t}^{ch} - \frac{P_{i,t}^{dch}}{\eta_i^{dch}} \quad , \ \forall t \geq 1 \tag{54}$$

$$E_{i,t,s} = E_i^{initial} \quad , t = 0 \tag{55}$$

$$U_{i,t}^{ch} + U_{i,t}^{dch} \leq 1 \tag{56}$$

- *Power balance for each MG:*

$$\begin{aligned} &\sum_{i \in MGp} \left(P_{i,t}^{PV} + P_{i,t}^{MT} + P_{i,t}^{dch} - P_{i,t}^{ch} \right) + P_t^{DSO2MGp} - P_t^{MGp2DSO} + P_t^{Rw2MGp} + \\ &\sum_{q=1, q \neq p}^{N_{MG}} \left(P_t^{MGq2MGp} - P_t^{MGp2MGq} \right) = \sum_{i \in MGp} (P_{i,t}^{L}) \end{aligned} \tag{57}$$

$$P_t^{MGp,bid} = P_t^{Rw} + \sum_{q=1, q \neq p}^{N_{MG}} \left(P_t^{MGq2MGp} \right) \tag{58}$$

$$P_t^{MGp,offer} = - \sum_{q=1, q \neq p}^{N_{MG}} \left(P_t^{MGp2MGq} \right) \tag{59}$$

where, in the bidding strategy, $P_t^{MGp,bid}$ has a positive value and in the offering strategy, $P_t^{MGp,offer}$ has a negative value.

- *DR program limits:*

In this paper, incentive-based DR programs as bid-quantity package offers which include the incentive prices and related amount of load curtailment are implemented [16]. A typical bid-quantity package offer for the *i*th bus is formulated as follows:

$$H_{i,\min} \leq h_{i,\xi} \leq H_{i,\xi} \quad , \ \xi = 1 \tag{60}$$

$$0 \leq h_{i,\xi} \leq (H_{i,\xi+1} - H_{i,\xi}) \quad , \ \xi = 2,3,...,\varphi \tag{61}$$

$$P_i^{DR} = \sum_{\xi=1}^{\varphi} h_{i,\xi} \tag{62}$$

4.2.2. Lower-level of the SP: maximizing the social welfare

The maximum social welfare of the retail market clearing process including the consumers, producers, and retailers is derived by (63).

$$\underset{t \in T}{Max} \left\{ \sum_{p=1}^{N_{MG}} (\lambda_{p,t}^{MG} P_{t,cleared}^{MGp,bid} + \lambda_{p,t}^{MG} P_{t,cleared}^{MGp,offer}) - \sum_{w=1}^{N_{retailer}} \lambda_t^{Rw} P_t^{Rw} \right\} \tag{63}$$

where, $\lambda_{p,t}^{MG} P_{t,cleared}^{MGp,bid}$ and $\lambda_{p,t}^{MG} P_{t,cleared}^{MGp,offer}$ stand for the consumer and producer benefit if the *p*th MG act as a consumer and producer in the retail electricity market during period *t*, respectively. The value of clearing quantity in the bidding strategy is positive for consumer MG, while negative values are assigned in the offering strategy for producer MG. The last term of (63) represents the production cost of traditional retailers.

Constraints:

The lower-level objective function (63) subjects to the following constraints:

- *Preserving the profit of each retailer:*

$$\sum_{t=1}^{24} \rho_t^{RM} P_t^{Rw} - \sum_{t=1}^{24} \rho_t^{WM} P_t^{Rw} \geq 0 \tag{64}$$

Non-equality (64) preserves the profit of each retailer during the retail market clearing process, where it states that the income of retailer *w* for the sold power to the retail market should be more than the payments to the wholesale market for the purchased power.

- *Bid/offer price limitation:*

$$\lambda_{p,t}^{MG} \leq \lambda_{p,\max}^{MG} \tag{65}$$

$$\lambda_{w,t}^{R} \leq \lambda_{w,\max}^{R} \tag{66}$$

Equations (65)-(66) consider the bid/offer price caps in the retail electricity market for the *p*th MG and *w*th retailer at time *t*.

- *Relationship between bid/offer quantity and clearing quantity:*

$$\begin{cases} P_t^{MGp,offer} \leq P_{t,cleared}^{MGp,offer} < 0 & if \quad MGp \ is \ in \ the \ offering \ strategy \\ P_t^{MGp,bid} = P_{t,cleared}^{MGp,bid} & if \quad MGp \ is \ in \ the \ bidding \ strategy \end{cases} \tag{67}$$

Equation (67) states the relationship between bid/offer quantity and clearing quantity for each MG in the retail market. If *p*th MG acts as a producer (i.e., for the offering strategy) at time *t*, it is possible that its offer quantity will be fully satisfied, partially satisfied, or not satisfied. On the other hand, if *p*th MG acts as a consumer (i.e., for the bidding strategy) at time *t*, then its offer quantity should be fully accepted under any condition.

4.3. Solution methodology

In this paper, as stated before, a Nash equilibrium between a set of competing players (MGs) considering DR actions in the retail and wholesale electricity market is modeled. Fig. 1, briefly represents the high-level schematic overview of the proposed modelling framework and its transformation into a single-level MISOCP problem including four steps. First step shows the bi-level MP and SP including the related objective functions and constraints. The proposed bi-level model cannot be directly solved in the commercial solvers. To resolve this, in the second step, by implementing the KKT conditions for the lower-level of the SP, it is converted into a bi-level optimization problem. In the next level, by adding the lower-level optimality conditions of the MP, a single-level Mathematical Programming with Equilibrium Constraints (MPEC) problem is resulted. In the last step, by implementing the linearization techniques including the dual theory, auxiliary variables, and big-M disjunctive inequalities, the resulted MPEC problem is converted into an MISOCP problem, which can be solved by off-the-shelf software, such as CPLEX and GUROBI. In order to verify that each final solution yielded from the MISOCP problem is indeed a Nash equilibrium, a single-iteration diagonalization technique [29] is utilized. In this way, the optimization problem of each MG (i.e., player) is solved by holding the constant decision strategies for the remaining rival MGs (i.e., rival players). This process should be repeated for all of the N_{MG} MGs. If the resulted decision strategies are identical to those obtained by MISOCP problem, this means that no player has a profitable unilateral deviation, and that the final solution is a Nash equilibrium.

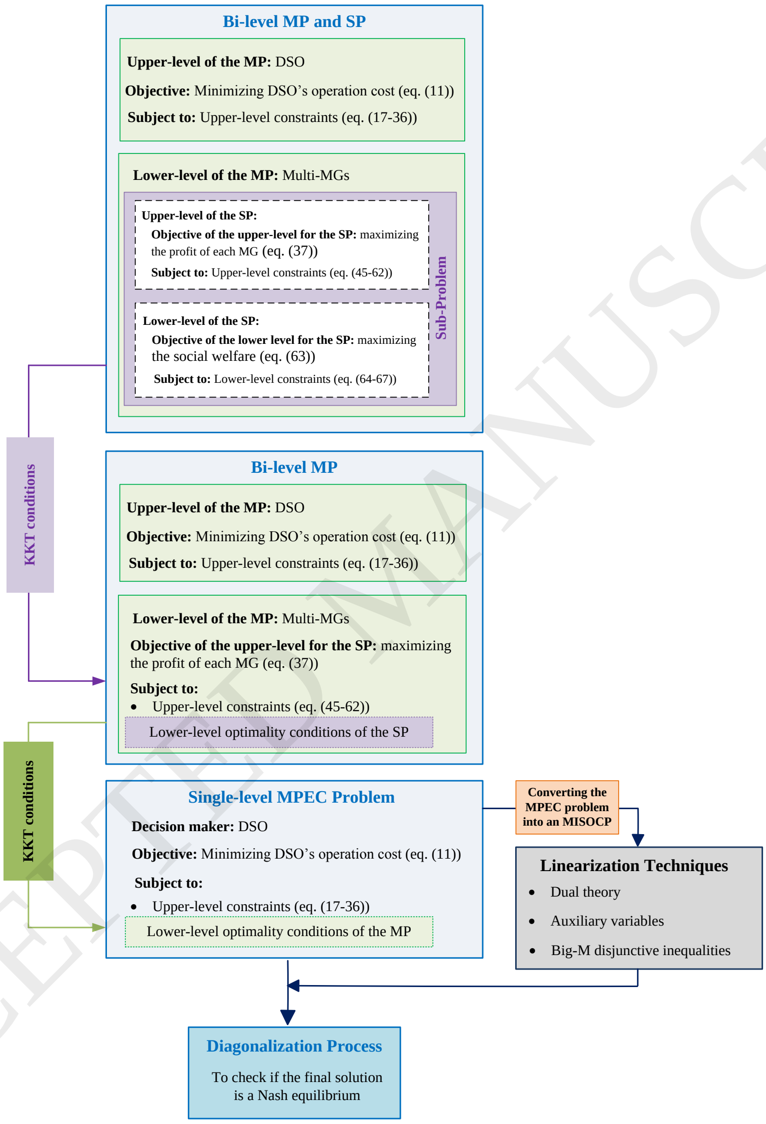

Fig. 1. Problem statement and its transformation from a bi-level problem into a single-level MISOCP problem

5. Test and results

In the previous sections, the bi-level framework of the MP and SP and the solution methodology were proposed. In this section, after introducing the case study, simulation results of the proposed model are discussed.

5.1. Case study

The 84-bus 11.4 kV Taiwan Power Company (TPC) distribution system [30], as shown in Fig. 2, is used to demonstrate the effectiveness of the proposed model. The considered radial distribution system includes three MGs which are interconnected via 13 tie switches. Moreover, it has 20 sectionalizing switches (normally-open switches) and 11 feeders. For the considered combined overhead and underground distribution system, lines 1-3, 17-20, 30-34, 47- 49, 54, 58-61, 73-74, and 77-81 are overhead, whereas the others are underground cables. Considering the location of the switches, both the structural changes in each MG and changes in connection points among MGs are possible. The sitting layout of MTs, Photovoltaics (PVs), and ESSs with a similar type and size are depicted in Fig. 2. The predicted amounts for PV output powers and the wholesale market prices for the whole 24-h scheduling horizon can be found in [31] and [30], respectively. All the technical parameters and characteristics of DERs are represented in Table 1 [30]. The hourly load profile of each MG during the 24-h time horizon is shown in Fig. 3. Fig. 4 shows the hourly solar radiation and wind speed data [21], which are used for the DLR calculations. Moreover, hourly ambient temperature and other required data for the DLR calculations can be found in [21]. The step-wise bid-quantity offer packages of the DR programs for the corresponding MGOs and their support areas are listed in Table 2 and Table 3, respectively. The proposed optimization problem is implemented in GAMS 24.5 and solved by the CPLEX solver [32].

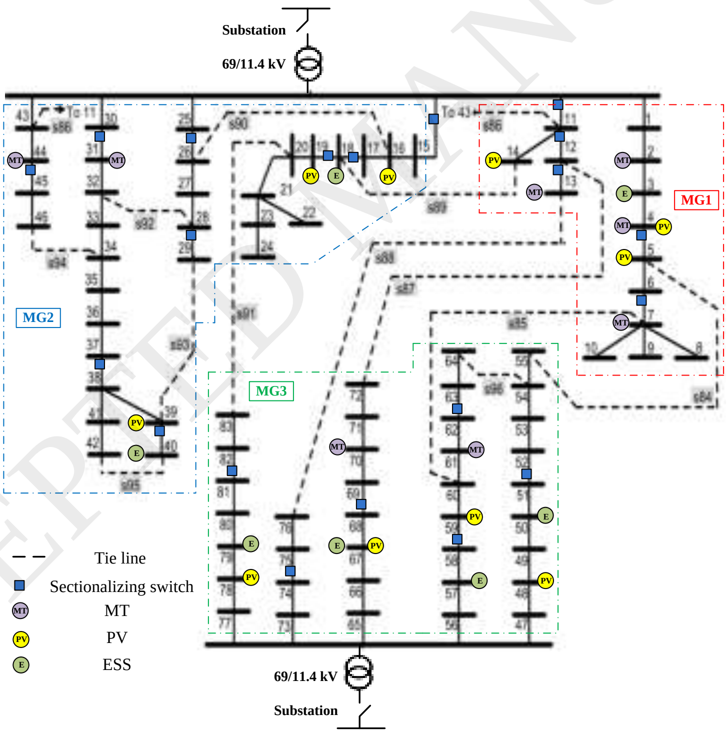

Fig. 2. 84-bus TPC distribution system [30]

Table 1. Values for technical parameters [30]

Parameter	Value	Parameter	Value
ρ^{loss} ($\$/MWh$)	400	α_i^{MT} ($\$/MWh$)	65
ρ^{SW} ($\$$)	1	β_i^{MT} ($\$$)	13
$P_{\max}^{MGp2DSO}$ / $P_{\max}^{DSO2MGp}$ (MW)	20	α_i^{PV} ($\$/MWh$)	1.3
$P_{\max}^{MGp2MGq}$ / $P_{\max}^{MGq2MGp}$ (MW)	20	β_i^{PV} ($\$$)	5

$P_{\max}^{WM2DSO} / P_{\max}^{DSO2MG} (MW)$	36	α_i^{ESS} ($\$/MWh$)	2
$I_{i,j,max} (kA)$	1.8	β_i^{ESS} ($)	2.5
$V_{min}, V_{max} (p.u.)$	0.95, 1.05	$N_{\max}^{SW}$	8
$P_{\min}^{MT}, P_{\max}^{MT} (MW)$	0, 5	$P_{\min}^{ESS}, P_{\max}^{ESS} (MW)$	1
$E_{\min}, E_{\max} (MWh)$	0.5, 2	$\eta_i^{ch}, \eta_i^{dch} (p.u.)$	0.92, 0.92
$\lambda_{p,\max}^{MG}$ ($\$/MWh$)	200	$\lambda_{w,\max}^{R}$ ($\$/MWh$)	200

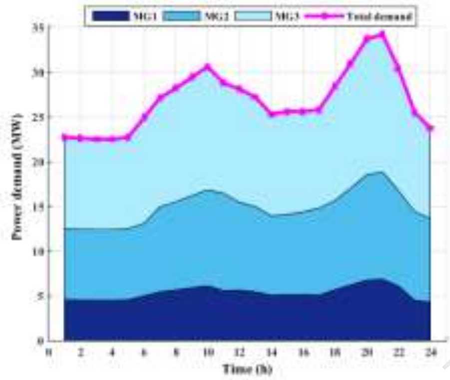

Fig. 3. Load profile of each MG [30]

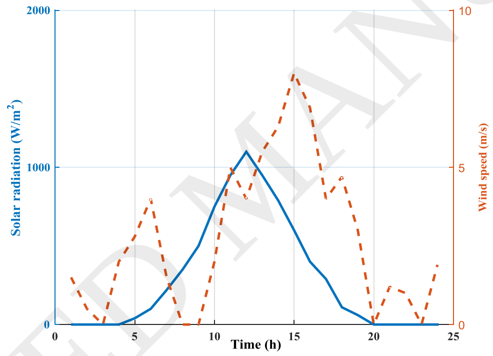

Fig. 4. Hourly solar radiation and wind speed [21]

Table 2. Bid quantity offer packages of DR programs [16]

MGO No.	DR Program [Quantity* (MW) & Price** ($/MWh)]			
MGO1	0-0.2* 94**	0.2-0.5 97	0.5-0.7 102	0.7-1.2 112
MGO2	0-0.2 91	0.2-0.8 97	0.8-1.4 104	1.4-1.8 116
MGO3	0-0.2 92	0.2-0.8 96	0.8-1.7 102	1.7-2.6 114

Table 3. Supported areas of DR programs for each MGO [16]

DR program	Buses
MG1	1, 4, 6, 7, 8, 13
MG2	16, 18, 21, 23, 28, 31, 32, 37, 40, 45
MG3	49, 50, 54, 59, 62, 63, 67, 68, 72,74, 78, 81, 82

5.2.Simulation results

In order to investigate the satisfactory performance of the proposed scheduling framework, the following case studies are considered:

Case Study 1 (CS1): Grid connected MGs, with DLR constraint, no reconfiguration

Case Study 2 (CS2): Grid connected MGs, with DLR constraint, with reconfiguration

Case Study 3 (CS3): Islanded MGs, no DLR constraint, no reconfiguration

Case Study 4 (CS4): Islanded MGs, with DLR constraint, no reconfiguration

Case Study 5 (CS5): Islanded MGs, with DLR constraint, with reconfiguration

To investigate the effect of wholesale market price variations on these case studies, three different scenarios are also defined. The base wholesale market prices proposed in [30], are assumed as scenario 1, where 10% decrement and increment in these prices are considered as scenario 2 and scenario 3, respectively. The simulation results and discussions are presented in the remainder of this section.

- ***CS1:***

As defined, there exists no reconfiguration process, thus all the tie switches are remained open in CS1. Accordingly, the power is not exchanged among MGs and there is no retail electricity market. Fig. 5 depicts the amount of exchanged power between each MG and DSO in different scenarios for CS1 over the day horizon. To ensure the economical operation of the distribution system, in off-peak load periods (i.e., 1:00-7:00) MG1 purchases power from DSO in all the scenarios, while it sells power to the DSO in other hours. Due to the shortage of power supply in MG3 in most of the times, MG operator 3 mainly acts as a purchaser. However, it sells the excess power to the DSO just in the hours with the highest PV power generation rates (i.e., at time 10:00-14:00). Due to the lower wholesale market prices in scenario 2, the amount of power sold by DSO to the MG operators is increased by 3% and 5%, respectively in comparison with the results of scenario 1 and scenario 3. Despite considering DLR constraint in CS1, feasible solution is obtained.

- ***CS2:***

The optimal open/close status of each RCS through the hourly reconfiguration in CS2 is presented in Table 4. As can be seen, RCS no. 52 has the most number of switching actions during the scheduling time, four times, which meets the maximum allowable number of switching limit.

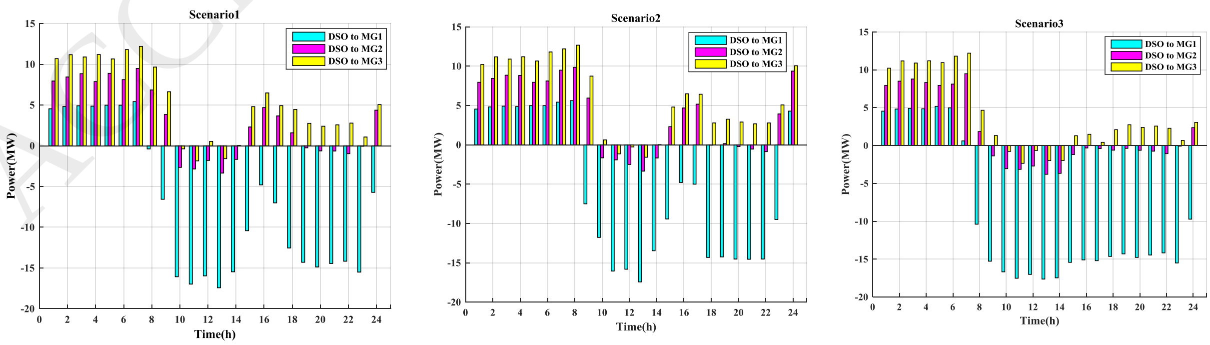

Fig. 5. Exchanged power between each MG and DSO in different scenarios for CS1

Fig. 6 shows the cleared retail electricity market prices in different scenarios for CS2. Due to the lower offers submitted by PV units in the market, the cleared prices at time 11:00-16:00 are decreased significantly. Moreover, in accordance with the decreased wholesale market prices in scenario 2, the cleared retail prices are decreased in comparison with that of scenario 1. Likewise, the cleared retail prices in scenario 3 are increased, which states the effect of wholesale market prices on the retail market clearing process. Hourly operation scheduling of the MTs, DR programs, and ESSs for CS2 in MG1, MG2, and MG3 are presented in Fig. 7, Fig. 8, and Fig. 9, respectively. As can be seen in scenario 2 for all the MGs, due to the decreased wholesale market prices, and thus decrement in retail market prices, as stated in Fig. 6, the amount of MTs output power and responsive load participations are decreased. Likewise, MTs output power and the amount of participated load in DR programs are increased in scenario 3 for all three MGs. Moreover, the charging/discharging schedules of ESSs state that they are charged during the off-peak periods and discharged (i.e., negative values in the figures) during the peak periods with higher electricity prices for all the scenarios.

Table 4. Opened RCSs in CS2

Hour	Open RCSs	Hour	Open RCSs
1-8	84-85-86-87-88-89-90-91-92-93-94-95-96	15-18	18-52-85-86-87-88-90-91-92-93-94-95-96
9-10	52-85-86-87-88-89-90-91-92-93-94-95-96	19-22	69-82-84-85-86-88-89-90-92-93-94-95-96
11-14	84-85-86-87-88-89-90-91-92-93-94-95-96	23-24	84-85-86-87-88-89-90-91-92-93-94-95-96

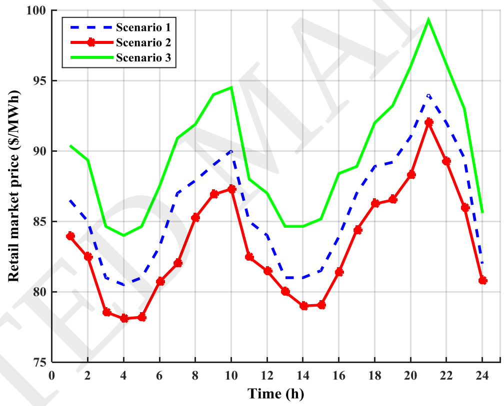

Fig. 6. Cleared retail market prices in different scenarios for CS2

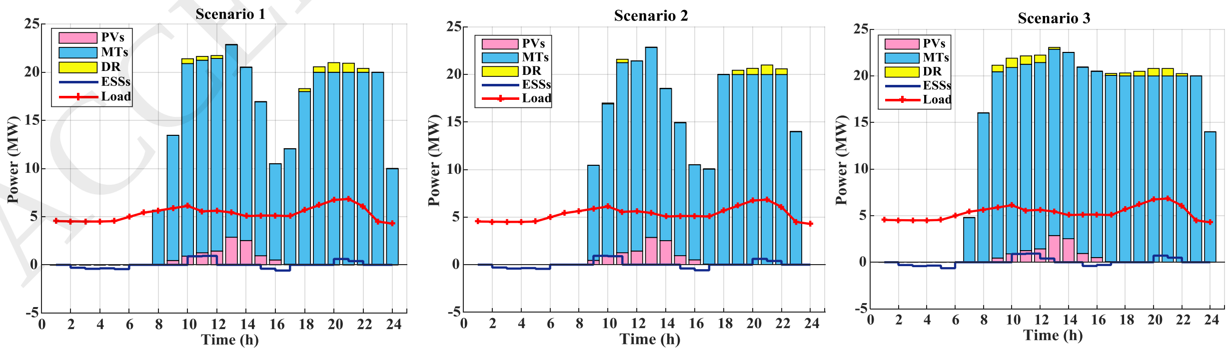

Fig. 7. Hourly operation scheduling of the MTs, DR programs, and ESSs in MG1 for CS2

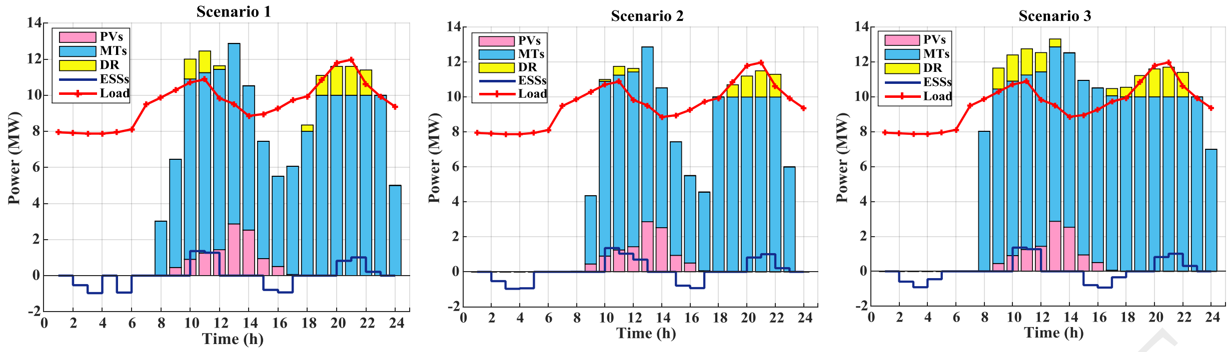

Fig. 8. Hourly operation scheduling of the MTs, DR programs, and ESSs in MG2 for CS2

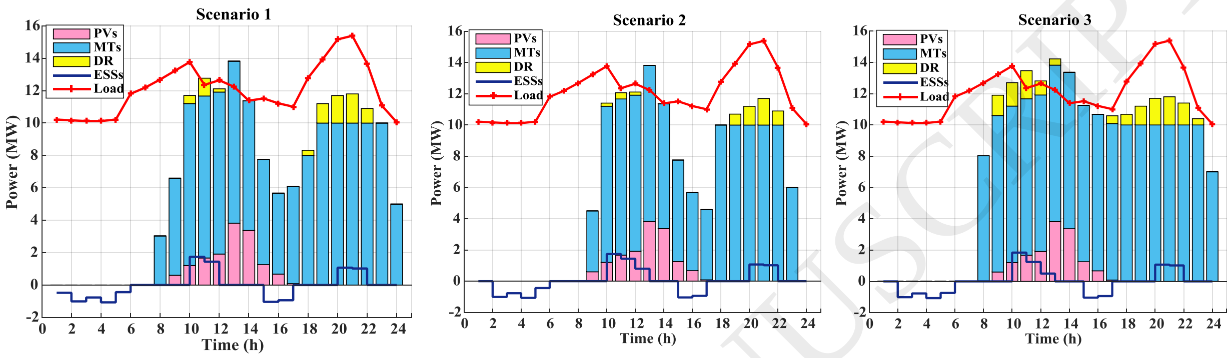

Fig. 9. Hourly operation scheduling of the MTs, DR programs, and ESSs in MG3 for CS2

The scheduled exchanged power between DSO and each MG in CS2 are illustrated in Fig. 10a. Moreover, Fig. 10b shows the amount of exchanged power among MGs in CS2 for all three scenarios. Due to the shortage of power in MG3, the power is transmitted from DSO, MG1, and MG2 to MG3 during most hours of the day. MG3, however, sells the power to the DSO just in the hours with the highest PV power generation rates (i.e., 10:00-14:00). On the other hand, because of the high penetration level of MTs and ESSs in MG1, it acts as a seller entity. As can be seen in Fig. 10b, due to the high-load level condition at time 16:00-21:00, the amount of transmitted power from MG1 to MG3 is increased significantly. The increment in purchased power from DSO in scenario 2 is particularly noteworthy. This amount is increased by 6% and 9%, respectively in comparison with those in scenario1 and scenario 3, which is mainly due to the lower electricity market prices in scenario 2. As feasible solution is obtained in CS1, it is obvious that by considering hourly reconfiguration and DLR constraint in CS2 feasible solution is reached as well.

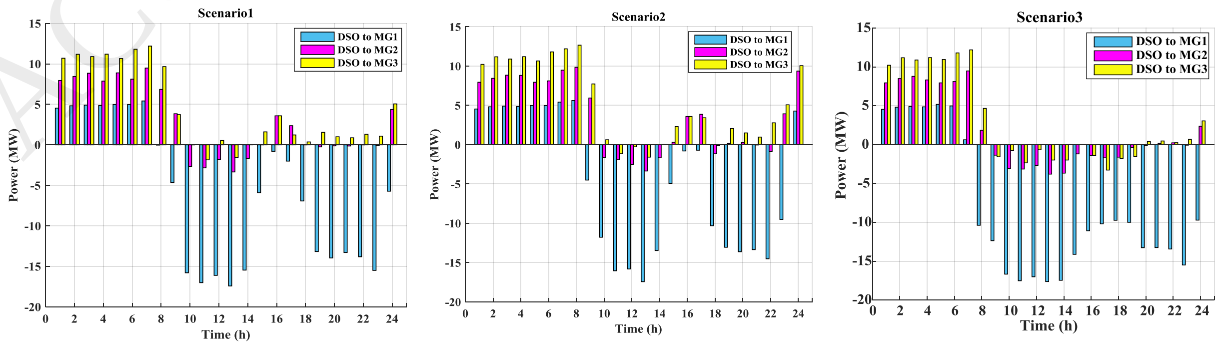

(a)

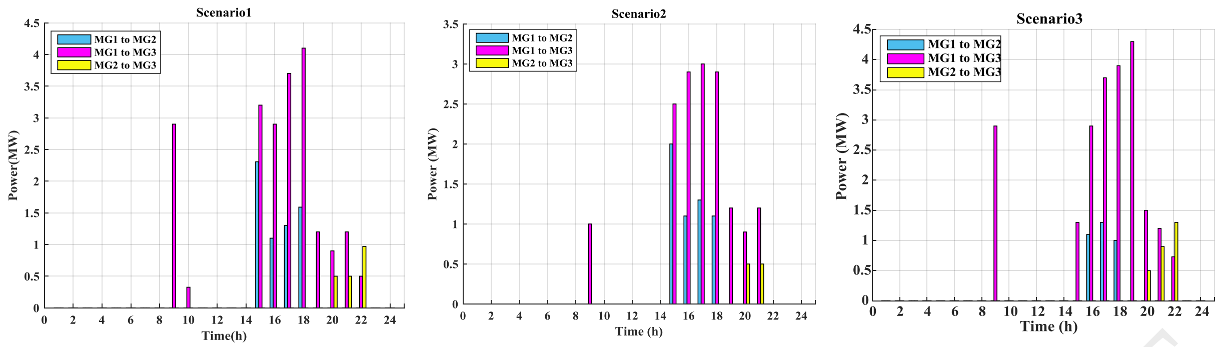

(b)

Fig. 10. Exchanged power in CS2 (a): between DSO and each MG, (b): among MGs

- ***CS3:***

Due to the defined islanded condition in CS3, CS4, and CS5, the wholesale market price variations in scenario 2 and scenario 3 does not influence the hourly operation scheduling of DERs. Therefore, in these case studies, the simulation results are provided just for scenario 1. Optimal operation scheduling of the MTs, DR programs, and ESSs for CS3 in the MGs are shown in Fig. 11. Likewise the previous case studies, ESSs are charged during the off-peak periods with lower market prices and discharged (i.e., negative values in the figures) during the peak periods with higher electricity prices for all the MGs. Moreover, PVs are operated at the corresponding maximum power generation points due to their lowest operation cost. As can be observed, the curtailable loads are participated in DR programs at the maximum allowable level in MG3 during most hours of the scheduled day, which is increased by 89% and 81%, respectively in comparison with those in CS1 and CS2. This is because the MGs are operated in islanded mode and there exists no reconfiguration process. So, the power shortage can be supplied neither by the DSO nor by the neighboring MGs.

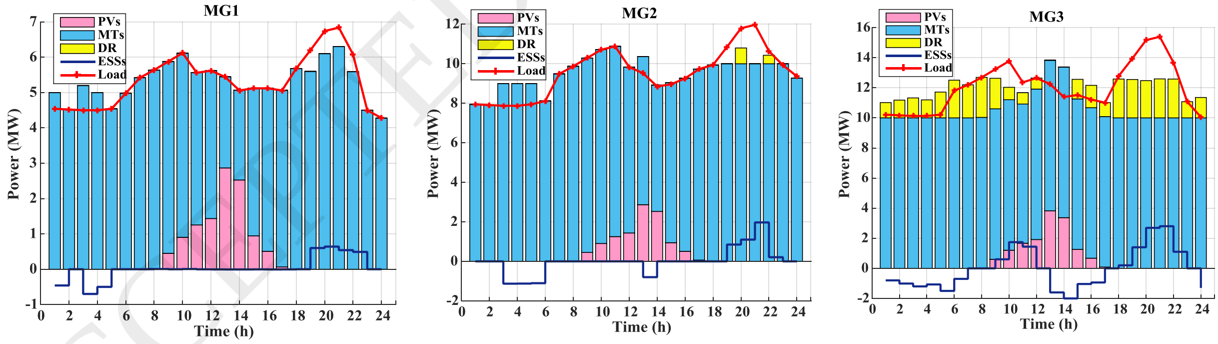

Fig. 11. Hourly operation scheduling of the MTs, DR programs, and ESSs in the MGs for CS3

- ***CS4:***

This case study considers the islanded MGs under the DLR constraint effect. Unlike the previous case study, by implementing DLR constraint into the model, power flow constraints demonstrate that lines 32, 47, and 59 are overloaded at peak time periods, and thus, there exists no feasible solution. To overcome this constraint violation, the hourly reconfiguration process is considered in CS5. In this regard, by optimally changing the status of tie and sectionalizing switches, new current paths are provided and load shedding is prevented.

- ***CS5:***

CS5 is defined to overcome the introduced challenge of considering DLR constraint in CS4 by utilizing hourly reconfiguration in short-term operation scheduling problem of the distribution system. To this end, by changing the status of RCSs, as reported in Table 5, the load current is distributed appropriately through the existing lines, thus preventing them to approach their maximum ampacity. It can be observed that by employing hourly reconfiguration, the capacity of violated lines are released and the networked MGs in islanded mode are operated at a feasible operating point. RCS no.52 has the most number of switching actions during the scheduled day, 6 times, which satisfies the maximum allowable number of switching limit. The cleared retail electricity market prices for CS5 is presented in Fig. 12. It is calculated that the average prices are increased by 12% in comparison with those in scenario 1 of CS2. This increment is mainly because of the islanded condition of the MGs, where the available energy is less than that of in the grid-connected mode. Similar to CS2, two valleys can be seen in Fig. 12, where the first one (i.e., during the time 2:00-6:00) is due to the low-load level condition, and the second one (i.e., during the time 12:00-16:00) is due to the lower offers submitted by PV units in the market.

Table 5. Opened RCSs in CS5

Hour	Open RCSs	Hour	Open RCSs
1-2	84-85-86-87-88-89-90-91-92-93-94-95-96	16-18	18-52-85-86-87-88-90-91-92-93-94-95-96
2-6	52-85-86-87-88-89-90-91-92-93-94-95-96	18-19	69-82-84-85-86-88-89-90-92-93-94-95-96
6-9	75-84-85-86-87-89-90-91-92-93-94-95-96	20-21	18-52-85-86-87-88-90-91-92-93-94-95-96
10-15	84-85-86-87-88-89-90-91-92-93-94-95-96	22-24	75-84-85-86-87-89-90-91-92-93-94-95-96

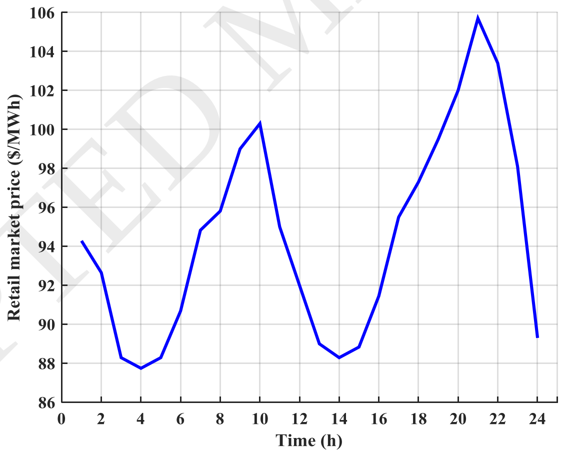

Fig. 12. Cleared retail market prices for CS5

Fig. 13 shows the Hourly operation scheduling of the MTs, DR programs, and ESSs in the MGs for CS5. The same as the previous case studies, ESSs store the excess energy during the off-peak periods, and they are discharged during the high market price periods to achieve more economic savings. In comparison with CS3, the total RL participation in DR programs is decreased around 42%, which is due to purchasing power from neighboring MGs with lower retail prices than the contracted bid prices of RLs. The amount of exchanged power among the MGs in CS5 is presented in Fig. 14. Due to the shortage of power in MG3 and excess generation capacity in MG1, the power is transmitted from MG1 to MG3 most of the times in the day.

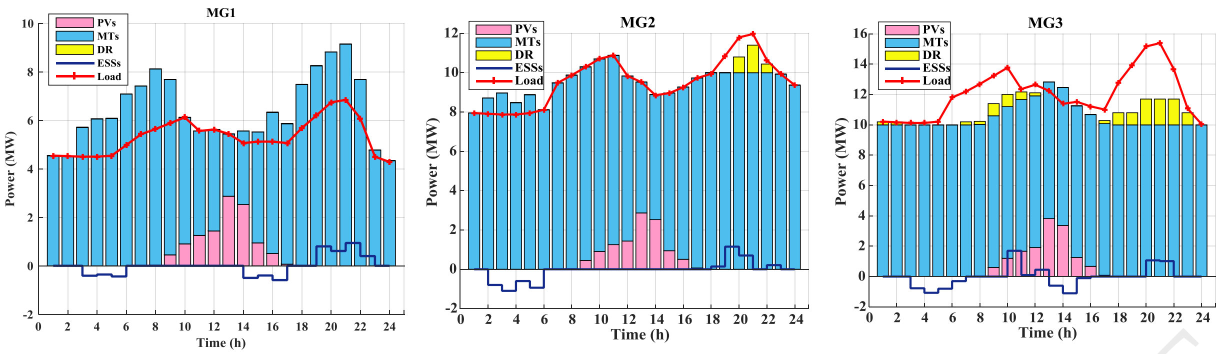

Fig. 13. Hourly operation scheduling of the MTs, DR programs, and ESSs in the MGs for CS5

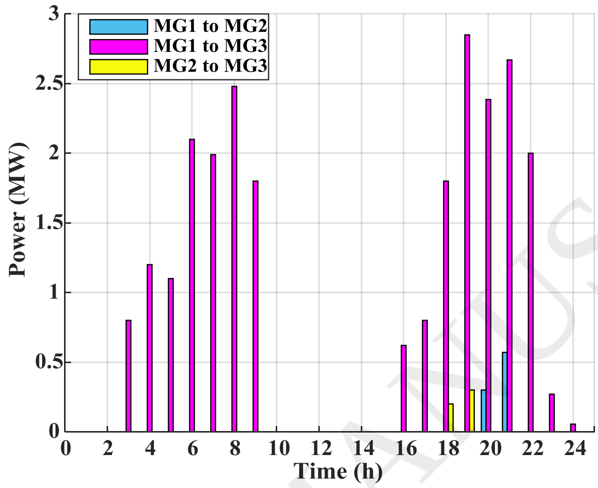

Fig. 14. Exchanged power among the MGs for CS5

Fig. 15 shows the total power loss of the system for different case studies over the scheduling time horizon. As can be seen, compared to CS1 and CS5, by implementing hourly reconfiguration in CS2 and CS4, the total power loss is decreased significantly, which has been introduced in the previous studies as one of the main applications of the reconfiguration technique. By relying on the own-based distributed generations such as MTs in islanded modes (i.e., CS3 and CS5), the amount of total power loss is decreased roughly by 17% in comparison with that of grid-connected mode (i.e., CS1 and CS2). Financial and technical comparison in different scenarios among the feasible four case studies are presented in Fig. 16. To reach a meaningful comparative study, the corresponding results of scenario 1 in CS1 is considered as 1.00 per unit (base values). As mentioned before, the wholesale market price variations in scenario 2 and scenario 3 does not influence the results of CS3 and CS5. Thus, the simulation results for all the three scenarios in these case studies are the same. For instance, it can be concluded that by utilizing the hourly reconfiguration in CS2, the RL participations in DR programs, profit of MG1, profit of MG2, and profit of MG3 in scenario 1 are increased by 9%, 3%, 3%, and 4%, respectively in comparison with those in CS1. Moreover, a reduction of 5% for total cost of the system in CS2 is achieved, which shows the effectiveness of the proposed networked MG structure and hourly reconfiguration process. Similarly, these promising results are achieved for both scenario 2 and scenario 3, by activating the hourly reconfiguration. It is shown that in the islanded MGs in CS3, the profit of all the MGs are decreased significantly as they are not able to provide power from DSO and neighboring MGs in the hours with lower market prices. By preparing the hourly reconfiguration and interconnections among the MGs in CS5, the profit of MGs are increased and the total system cost is decreased due to the stated reasons. Furthermore, in comparison with CS1, the responsive loads commitment in DR programs for CS3 and CS4 in scenario1 are increased around 27% and 31%, respectively. This increment is mainly happened because of the islanded condition of the MGs, where the available capacity of local suppliers are less than that of in the grid-connected mode. Thus, MGOs should rely on the RLs' participations more than other case studies. Table 6 displays the financial and technical advantages of deploying a retail electricity market in the distribution system. As can be seen, implementing the proposed retail electricity market environment could result in the increment of profit for MG1, MG2, and MG3 around 7%, 4%, and 8%, respectively. Moreover, the total cost of the system with retail market implementation is 72823, which shows 8% reduction in comparison with that of the model without retail market. Besides, it shows 3.2 MW more DR participations in the proposed model.

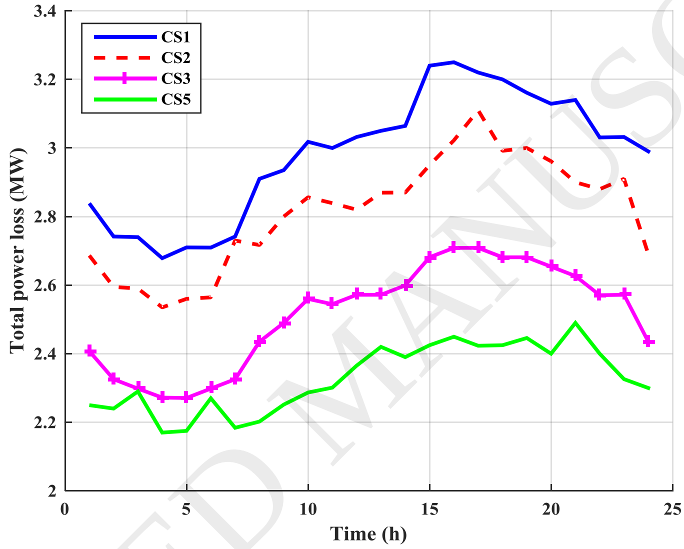

Fig. 15. Total power loss of the system for different case studies over the scheduling time horizon

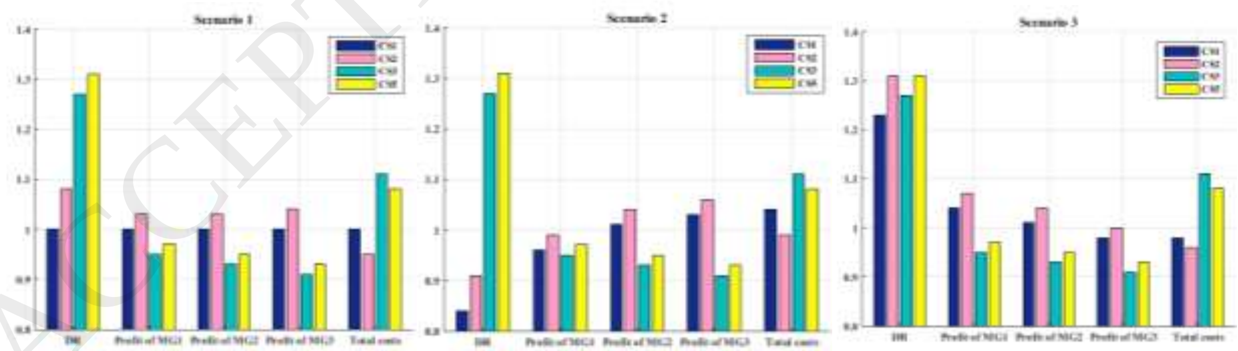

Fig. 16. Comparison of financial and technical results among different case studies

Table 6. Impact of market structure on the financial and technical results

Framework	DR participation (MW)	Profit of MG1 ($)	Profit of MG2 ($)	Profit of MG3 ($)	Total system cost ($)
With retail market	34.7	6381	4792	4027	72823

Without retail market	31.5	5934	4601	3704	78649

- **Computational efficiency analysis**

In order to investigate the scalability and efficiency of the proposed algorithm, beside the 84-bus TPC distribution system, larger distribution systems with 119 buses [33] and 1300 buses [34] are utilized. The first test system includes 5 MGs with 22.809 MW and 17.041 Mvar loads, where the second one includes 14 MGs with 132.074 MW and 115.269 Mvar loads. The required average calculation time of the algorithm for each test system are proposed in Table 7. As can be seen, the proposed algorithm reaches the optimal point within a reasonable running time, which illustrates the applicability of the algorithm for large scale systems.

Table 7. Computational efficiency analysis of the proposed algorithm

	84-bus TPC	IEEE 119-bus	IEEE 1300-bus
Calculation time (s)	25.3	31.1	97.4

- **Analysis on the Relaxation Exactness**

In order to evaluate the exactness of the obtained relaxed form in (24), the values in both sides of (24) must be nearly equal. In other words, in case that the left and right hand side of (24) are converged to each other, the obtained solution is authentic. Thus, to examine the relaxation exactness, the absolute relaxation gap for (24) is defined as follows:

$$\Delta_{ij,t}^{diff} = \left| \frac{P_{ij,t}^2 + Q_{ij,t}^2 - \ell_{ij,t} v_{i,t}}{P_{ij,t}^2 + Q_{ij,t}^2} \right| \qquad \forall\ (i,j) \in br \tag{68}$$

Fig. 17 shows the relaxation gap for the proposed MISOCP model. It can be seen that the calculated gap is very small, which demonstrates the relaxation exactness.

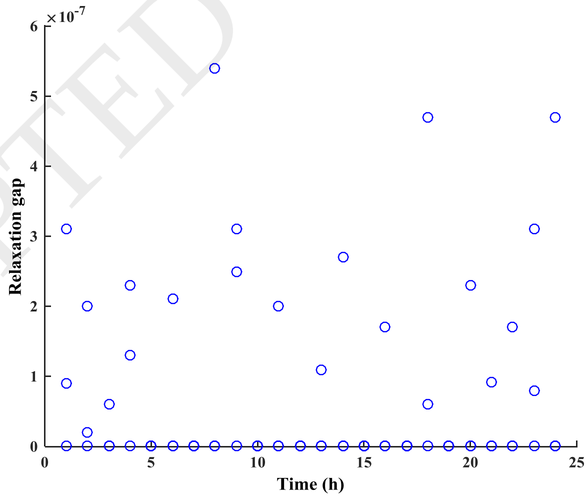

Fig. 17. Gap scatter for the proposed MISOCP model

6. Conclusion

This paper addressed the optimal operation scheduling problem of reconfigurable networked MGs complemented by demand response programs and DLR constraint. A multi-follower-type bi-level optimization scheduling was modeled to embody DSO-MGOs gaming strategy with inherently conflicting objectives. In the upper-level of the MP, the total system cost from

DSO's perspective is minimized, while in the lower-level of the MP, networked MGs compete with retailers in the retail electricity market as an interior SP. The upper-level of the SP sought to maximize the profit of each MG taking into account maximizing the social welfare of the retail market clearing process as the lower-level of the SP. To transform the non-linear bi-level optimization problem into a single-level MISOCP problem, KKT conditions and linearization techniques were implemented. The satisfactory performance of the proposed model was demonstrated on the 84-bus TPC distribution system as a real case study. It was shown that DLR constraint can effect maximum allowed line ampacity and some overloaded lines were detected in the islanded mode, which resulted in non-feasible solution. By optimally changing the status of tie and sectionalizing switches and providing new current paths though hourly reconfiguration process, this constraint violation was eliminated. Hourly reconfiguration not only prevented the presence of the overloaded lines in the distribution system, but also improved the total power losses, participation in DR programs, MGOs' profit, and the total cost significantly. Besides, by submitting price-quantity bids/offers of competing MGs and retailers in the established retail market, participation in DR programs, MGOs' profit, and the total system cost were improved. It was also observed that when the market prices are relatively higher, MGOs prefer to rely on their own DERs including MTs, PVs, and RLs and then exchange the possible surplus or shortage of power with neighboring MGs and DSO. However, in conditions where the market prices are lower, MGOs prefer to trade more with DSO.

References

[1] Boudoudouh S, Maâroufi M. Multi agent system solution to microgrid implementation. Sustainable Cities and Society. 2018 May 1;39:252-61.

[2] Silvente J, Papageorgiou LG. An MILP formulation for the optimal management of microgrids with task interruptions. Applied Energy. 2017 Nov 15;206:1131-46.

[3] Esmaeili S, Jadid S. Economic-Environmental Optimal Management of Smart Residential Micro-Grid Considering CCHP System. Electric Power Components and Systems. 2019 Jan 27:1-5.

[4] Zhang Y, Meng F, Wang R, Zhu W, Zeng XJ. A Stochastic MPC based Approach to Integrated Energy Management in Microgrids. Sustainable Cities and Society. 2018 May 24.

[5] Nikmehr N, Ravadanegh SN. Optimal power dispatch of multi-microgrids at future smart distribution grids. IEEE Transactions on Smart Grid. 2015 Jul;6(4):1648-57.

[6] Li YZ, Zhao T, Wang P, Gooi HB, Wu L, Liu Y, Ye J. Optimal Operation of Multi-Microgrids via Cooperative Energy and Reserve Scheduling. IEEE Transactions on Industrial Informatics. 2018 Jan 12.

[7] Song NO, Lee JH, Kim HM, Im YH, Lee JY. Optimal energy management of multi-microgrids with sequentially coordinated operations. Energies. 2015 Aug 7;8(8):8371-90.

[8] Lv T, Ai Q, Zhao Y. A bi-level multi-objective optimal operation of grid-connected microgrids. Electric Power Systems Research. 2016 Feb 1;131:60-70.

[9] Wang Z, Chen B, Wang J. Decentralized energy management system for networked microgrids in grid-connected and islanded modes. IEEE Transactions on Smart Grid. 2016 Mar;7(2):1097-105.

[10] Jalali M, Zare K, Seyedi H. Strategic decision-making of distribution network operator with multi-microgrids considering demand response program. Energy. 2017 Dec 15;141:1059-71.

[11] Bahramara S, Moghaddam MP, Haghifam MR. Modelling hierarchical decision making framework for operation of active distribution grids. IET Generation, Transmission & Distribution. 2015 Dec 3;9(16):2555-64.

[12] Bahramara S, Moghaddam MP, Haghifam MR. A bi-level optimization model for operation of distribution networks with micro-grids. International Journal of Electrical Power & Energy Systems. 2016 Nov 1;82:169-78.

[13] Marzband M, Javadi M, Pourmousavi SA, Lightbody G. An advanced retail electricity market for active distribution systems and home microgrid interoperability based on game theory. Electric Power Systems Research. 2018 Apr 30;157:187-99.

[14] Zachar M, Daoutidis P. Microgrid/macrogrid energy exchange: A novel market structure and stochastic scheduling. IEEE Transactions on Smart Grid. 2017 Jan;8(1):178-89.

[15] Fu H, Zhang XP. Market Equilibrium in Active Distribution System With $\mu $ VPPs: A Coevolutionary Approach. IEEE Access. 2017;5:8194-204.

[16] Esmaeili S, Jadid S, Anvari-Moghaddam A, Guerrero JM. Optimal Operational Scheduling of Smart Microgrids Considering Hourly Reconfiguration. In2018 IEEE 4th Southern Power Electronics Conference (SPEC) 2018 Dec 10 (pp. 1-6). IEEE.

[17] Esmaeili S, Anvari-Moghaddam A, Jadid S, Guerrero J. A stochastic model predictive control approach for joint operational scheduling and hourly reconfiguration of distribution systems. Energies. 2018 Jul 19;11(7):1884.

[18] Farhudi T, Jannati Oskuee MR, Najafi Ravadanegh S. Multi-objective modelling of day ahead scheduling of MMG-based distribution networks accompanied by DEA considering economics, emissions and power quality. International Journal of Ambient Energy. 2018 Mar 2:1-2.

[19] Esmaeili S, Anvari-Moghaddam A, Jadid S, Guerrero JM. Optimal simultaneous day-ahead scheduling and hourly reconfiguration of distribution systems considering responsive loads. International Journal of Electrical Power & Energy Systems. 2019 Jan 1;104:537-48.

[20] Bhattarai BP, Gentle JP, McJunkin T, Hill PJ, Myers KS, Abboud AW, Renwick R, Hengst D. Improvement of Transmission Line Ampacity Utilization by Weather-Based Dynamic Line Rating. IEEE Transactions on Power Delivery. 2018 Aug;33(4):1853-63.

[21] Dabbaghjamanesh M, Kavousi-Fard A, Mehraeen S. Effective Scheduling of Reconfigurable Microgrids with Dynamic Thermal Line Rating. IEEE Transactions on Industrial Electronics. 2018 Apr 17.

[22] Fanelli V, Maddalena L, Musti S. Asian options pricing in the day-ahead electricity market. Sustainable Cities and Society. 2016 Nov 1;27:196-202.

[23] Li R, Wei W, Mei S, Hu Q, Wu Q. Participation of an Energy Hub in Electricity and Heat Distribution Markets: An MPEC Approach. IEEE Transactions on Smart Grid. 2018 May 4.

[24] Moreno B, Díaz G. The impact of virtual power plant technology composition on wholesale electricity prices: A comparative study of some European Union electricity markets. Renewable and Sustainable Energy Reviews. 2019 Jan 1;99:100-8.

[25] Michiorri A, Nguyen HM, Alessandrini S, Bremnes JB, Dierer S, Ferrero E, Nygaard BE, Pinson P, Thomaidis N, Uski S. Forecasting for dynamic line rating. Renewable and sustainable energy reviews. 2015 Dec 1;52:1713-30.

[26] IEEE Standard 738-2006. IEEE standard for calculating the current temperature relationship of bare overhead conductors. 2006.

[27] Li N, Chen L, Low SH. Exact convex relaxation of OPF for radial networks using branch flow model. In2012 IEEE Third International Conference on Smart Grid Communications (SmartGridComm) 2012 Nov 5 (pp. 7-12). IEEE.

[28] Farivar M, Low SH. Branch flow model: Relaxations and convexification—Part I. IEEE Transactions on Power Systems. 2013 Aug;28(3):2554-64.

[29] Pandžić K, Pandžić H, Kuzle I. Virtual storage plant offering strategy in the day-ahead electricity market. International Journal of Electrical Power & Energy Systems. 2019 Jan 1;104:401-13.

[30] Esmaeili S, Anvari-Moghaddam A, Jadid S. Optimal Operational Scheduling of Reconfigurable Multi-Microgrids Considering Energy Storage Systems. Energies. 2019 Jan;12(9):1766.

[31] Rabiee A, Sadeghi M, Aghaeic J, Heidari A. Optimal operation of microgrids through simultaneous scheduling of electrical vehicles and responsive loads considering wind and PV units uncertainties. Renewable and Sustainable Energy Reviews. 2016 May 1;57:721-39.

[32] CPLEX Optimization Subroutine Library Guide and Reference, ILOG Inc., Incline Village, NV, CPLEX division edn., 2008.

[33] Fan H, Duan C, Zhang CK, Jiang L, Mao C, Wang D. ADMM-Based Multiperiod Optimal Power Flow Considering Plug-In Electric Vehicles Charging. IEEE Transactions on Power Systems. 2018 Jul;33(4):3886-97.

[34] IEEE Test Feeders (accessed: Jan. 2018). [Online]. Available: https://ewh.ieee.org/soc/pes/dsacom/testfeeders/.